In situ [7]Li nuclear magnetic resonance study of the relaxation effect in practical lithium ion batteries

Kazuma Gotoh[a], Misato Izuka[a], Juichi Arai[b], Yumika Okada[b], Teruyasu Sugiyama[b],*

Kazuyuki Takeda[c], and Hiroyuki Ishida[a]

[a] Graduate School of Natural Science & Technology, Okayama University, 3-1-1

    Tsushima-naka, Okayama 700-8530, Japan

[b] Yamaha Motor Co., Ltd., 2500 Shingai, Iwata, Shizuoka 438－8501, Japan

[c] Division of Chemistry, Graduate School of Science, Kyoto University, Kyoto 606-8502,

    Japan

(Abstract)

Lithium ion cells comprising actual components of positive electrodes ($LiCoO_2$, $LiNi_xCo_yAl_z$, and $LiMn_2O_4$) and negative electrodes (graphite and hard carbon) were assembled for *in situ* [7]Li nuclear magnetic resonance (NMR) experiments. The ^{7}Li NMR measurements of the cells revealed a "relaxation effect" after overcharging: a decrease of the signal assigned to Li metal deposited on the negative electrode surface by overcharging. The reduction of the Li metal signal was inversely proportional to the increase of the signal of lithium stored in carbon. Therefore, the effect was ascribed to absorption of deposited

---

*Corresponding author. Tel/Fax: +81 86 251 7776

E-mail : kgotoh@cc.okayama-u.ac.jp (K. Gotoh)

lithium into the carbon of negative electrodes. The effect, which occurred rapidly in a few hours, reached an equilibrium state at 8–15 h. The slight shift of deposited metal suggests that dendritic Li easily re-dissolved, although larger Li particles remained. A hard carbon electrode has a greater effect of Li metal relaxation than graphite electrodes do, which is explainable by the bufferable structure of the carbon. Results are expected to be important for the discussion of the state of lithium, and for safer battery design.

---

1. Introduction

Lithium ion batteries (LIBs), a crucially important power source, are increasingly demanded for application to electrical devices and electric vehicles [1]. To improve the LIB capacity, efficiency, lifetime, and safety, it is indispensable to elucidate the states of the lithium atoms on the positive electrode (cathode) and on the negative electrode (anode). ^{6}Li/^{7}Li nuclear magnetic resonance (NMR) is suitable for characterizing LIBs because the spectra reflect the environment of the lithium atoms [2–5]. Particularly *in situ* NMR experiments of LIBs have been attracting interest because they allow for access to the non-equilibrium state of the battery during charging and discharging processes in a non-invasive manner [6–8]. To date, *in situ* NMR studies of LIBs for carbon electrodes [9–13], metal electrodes [14, 15], and lithium metal oxide electrodes [16–18] have been reported.

All previous studies have specifically addressed either one of the pair of electrodes using cells with a working electrode on one side and lithium metal electrode on the other side. However, for LIBs in actual use, what happens on the negative electrode can be

affected by the positive electrode material, and vice versa. For example, a $LiCoO_2$ electrode can provide more lithium ions than a $LiMn_2O_4$ electrode can. Such a difference in the positive electrode can affect the rate of lithium-metal deposition on the negative electrode when the battery is overcharged. It follows that *in situ* Li NMR of a "full cell" composed of the positive electrode and negative electrode used in practical and operational LIBs would be favorable, rather than analyses of the lithium environment on the positive and negative electrodes in separate samples of "half cells". To evaluate the overcharged state of LIBs accurately, well-designed full cells having appropriate balance of capacities in positive and negative electrodes are necessary.

This report describes *in situ* ^{7}Li NMR studies of full LIB cells using $LiCoO_2$, $LiNi_xCo_yAl_z$, and $LiMn_2O_4$ for the materials of positive electrode, and graphite and hard carbon for the materials of negative electrode. We fabricated cells for various combinations of these materials in a compact form that is suitable for *in situ* NMR. Then we measured ^{7}Li spectra for various states of charge (SOC). Results show that *in situ* ^{7}Li NMR analysis exhibits an interesting phenomenon of the deposited lithium on the negative electrode after overcharging: lithium metal is transferred into the carbon electrode material within a few hours. To date, such a relaxation effect has only been predicted. This report is the first to describe experimental evidence for the relaxation after overcharging. Results show that the hard carbon electrode can absorb more lithium atoms than the graphite electrode can. A discussion of the results will be given in terms of the pores that can be buffers of the lithium atoms.

2. Experimental

2.1 *Preparation of cells for NMR*

Cells sealed by Al-deposited laminate film were assembled for *in situ* measurements, with a positive electrode made with lithium transition metal oxides, a negative electrode made with carbon, and polypropylene separator (25 μm). The cells were filled with liquid electrolyte comprising 1 M $LiPF_6$ in ethylene carbonate (EC) / ethylmethylcarbonate (EMC) mixture with a volume ratio of 30:70. The positive electrode was prepared by coating an active material on an Al foil (20 μm). $LiCoO_2$ (LCO), $LiNi_xCo_yAl_z$ (x:y:z=8:2:<0.1) (NCA), or $LiMn_2O_4$ (LMO) was used as active materials. The capacity was precisely adjusted to 3.0 mAh cm^{-2}. The negative electrodes were formed on a Cu foil (18 μm thickness) in the same manner using an artificial graphite powder (20~30 μm of particle sizes) or pitch-based hard carbon (Carbotron PS(F), Kureha Battery Materials Japan). Characterization of the hard carbon product has been reported in [4] and [19]. Each negative electrode was prepared adjusting its capacity at 3.2 mAh cm^{-2} (corresponding to 360 mAh g^{-1} for graphite and 450 mAh g^{-1} for hard carbon). Each positive electrode and negative electrode was cut in rectangular shape (10 x 16 mm), and assembled to a cell. Thus, the capacity balance of negative against positive in each cell was same. The cell size was 30 mm × 20 mm, and the thickness of the Al-deposited laminate packing was 115 μm (the Al thickness in the laminate film was less than 30 μm). A schematic drawing of the cell is presented in Fig. 1(a).

To evaluate the reduction of the NMR signal attributable to radiofrequency (RF) shielding by the Al layer in the package, Li metal samples packed in the polyethylene

terephthalate (PET) film (100 μm thickness) and in the Al-deposited laminate film were fabricated. The results of the NMR measurements are described in the section 3.1.
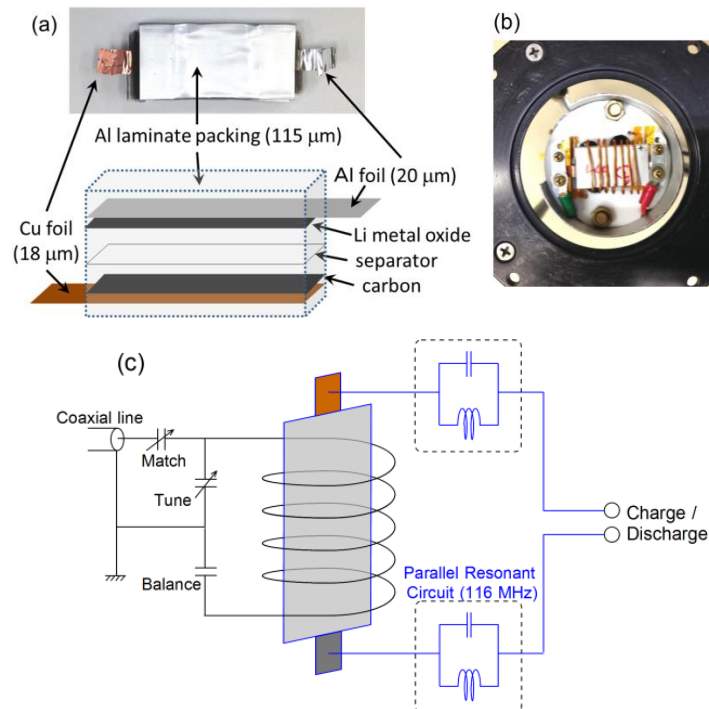

Fig. 1   Photograph and schematic drawing of a practical component cell for in situ NMR measurement (a), photograph of the cell set on the head of a NMR probe (b), and a schematic drawing of the NMR probe including isolation shunt circuit (c).

2.2 In situ NMR

In situ ^{7}Li NMR experiments were conducted using a 7 T superconducting magnet and a homebuilt NMR spectrometer [20]. For this study, we developed an in situ ^{7}Li NMR probe that can charge–discharge the cell while NMR experiments are performed (Fig. 1(b)). It is equipped with a flattened solenoid coil tuned at the [7]Li Larmor frequency (116.41 MHz) and a pair of terminal ports for charging–discharging. To isolate the RF circuit from

the charge–discharge circuit, a shunt pair of a capacitor and an inductor resonating at 116 MHz was attached to each of the two terminals, acting as a high-impedance trap at the NMR frequency, although it has a slight effect on direct currents. The cell was folded and put in the coil, and thereby in the magnet with the cell plane normal to the magnetic field. A single pulse sequence was applied with a pulse length of 6 μs corresponding to the 90 deg spin flip. The spectral width was 200 kHz, which was enough to observe all Li components. A ^{7}Li NMR signal in saturated aqueous solution of LiCl was used as a chemical shift reference. Although 50 ~ 100 scan was enough to observe each Li component, we accumulated 1000 scans to obtain good S/N ratio.

First, to estimate the effect of RF shielding by the Al layer, we compared [7]Li signal intensities of the samples sealed by the Al-deposited laminate and by the PET film. Then, the cells made with the LCO and graphite electrodes (LCO-gph), NCA and graphite (NCA-gph), LMO and graphite (LMO-gph), and LCO and hard carbon (LCO-hc) were subjected to the *in situ* ^{7}Li NMR studies. The cutoff potentials of the cell for the charge and discharge processes were, respectively, 4.20 V and 2.75 V (2.5 V for LCO-hc). The cell was charged–discharged by 0.5 C (3–4 mA) for each sample.

In general, cells can be charged efficiently using the CC–CV method: the cell is charged rapidly by the constant current (CC) mode; then it is charged slowly by the constant voltage (CV) mode. However, such precise control is difficult when the cell is accidentally overcharged during actual use. Accordingly, we applied CC charging without the CV process for all samples. 100% SOC was experimentally defined by the first

6

discharged capacity after formation process (4.5 mAh for graphite cells, and 3.5 mAh for hard carbon cells).

2.3 Observation of absorption effects of Li metal into carbon

LCO-gph, NCA-gph, LMO-gph, and LCO-hc cells were applied to the experiment. The cells were overcharged to 170% of SOC by 2 C (until ca. 4.9 V) for LCO-gph, NCA-gph, and LMO-gph cells, and to 170% of SOC by 3 C (until ca. 4.9 V) for LCO-hc cell. After the overcharging, NMR spectra were immediately measured every 17 min.

3. Results and Discussion

3.1 *Estimation of shielding effect by Al-laminate film and Cu foil*

The ^{7}Li NMR signals of Li metal packed in the PET film and in the Al-deposited laminate film are presented in Fig. 2(a). Results showed that the signal intensity was attenuated by ca. 50% attributable to RF shielding by the aluminum layer in the laminate film. Signals of Li metal with electrolyte solution and of Li metal electrode (Li pasted on Cu foil (18 μm thickness) with electrolyte solution are also presented for comparison in Fig. 2(b). The signal intensity decreased by 20–30% by the Cu foil. Although the signals were weakened by the Al-laminate film and Cu foil in the battery, we observed 35–40% intensity of the signal, which is tolerable for our study. Actually, RF wave can pass metal layer only less than 10 μm. Therefore, the NMR signals must be obtained from the "edge" parts of the cells and come out through voids between deposited Aluminum particles in laminate film. To avoid the RF shielding effect, Cu and Al meshes were used for the electrodes in

previous studies [6, 10, 16]. However, metal foils and laminated packing by thicker Al film are preferred to maintain cell stability for a long time. The assembled cells in this study were stable; no disintegration of the components was found over three months. The cells were used for the following ^{7}Li *in situ* NMR experiments.
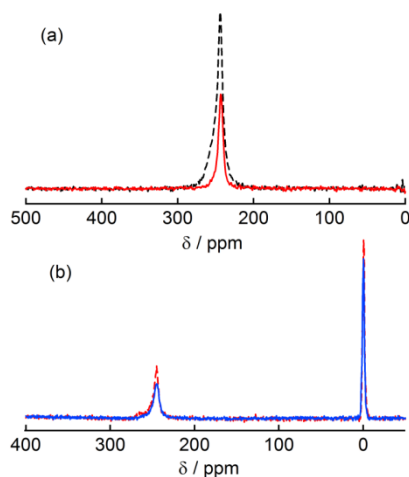

Fig. 2   Signals of Li metal in PET film (black broken line) and in Al-deposited laminate film (red solid line) (a). Li metal with electrolyte solution (red broken line) and Li metal electrode (Li pasted on Cu foil) with electrolyte solution (blue solid line) (b).

3.2 ^{7}Li NMR

Figures 3(a)–3(d) respectively show ^{7}Li NMR spectra of LCO-gph, NCA-gph, LMO-gph, and LCO-hc cells in the range of +100 and -30 ppm (+150 and -50 ppm for (c)). Spectrum of wider range (between +400 and -200 ppm) and the discharge curve of each cell are shown in Fig. S1 and S2, respectively, in a supplementary material file.
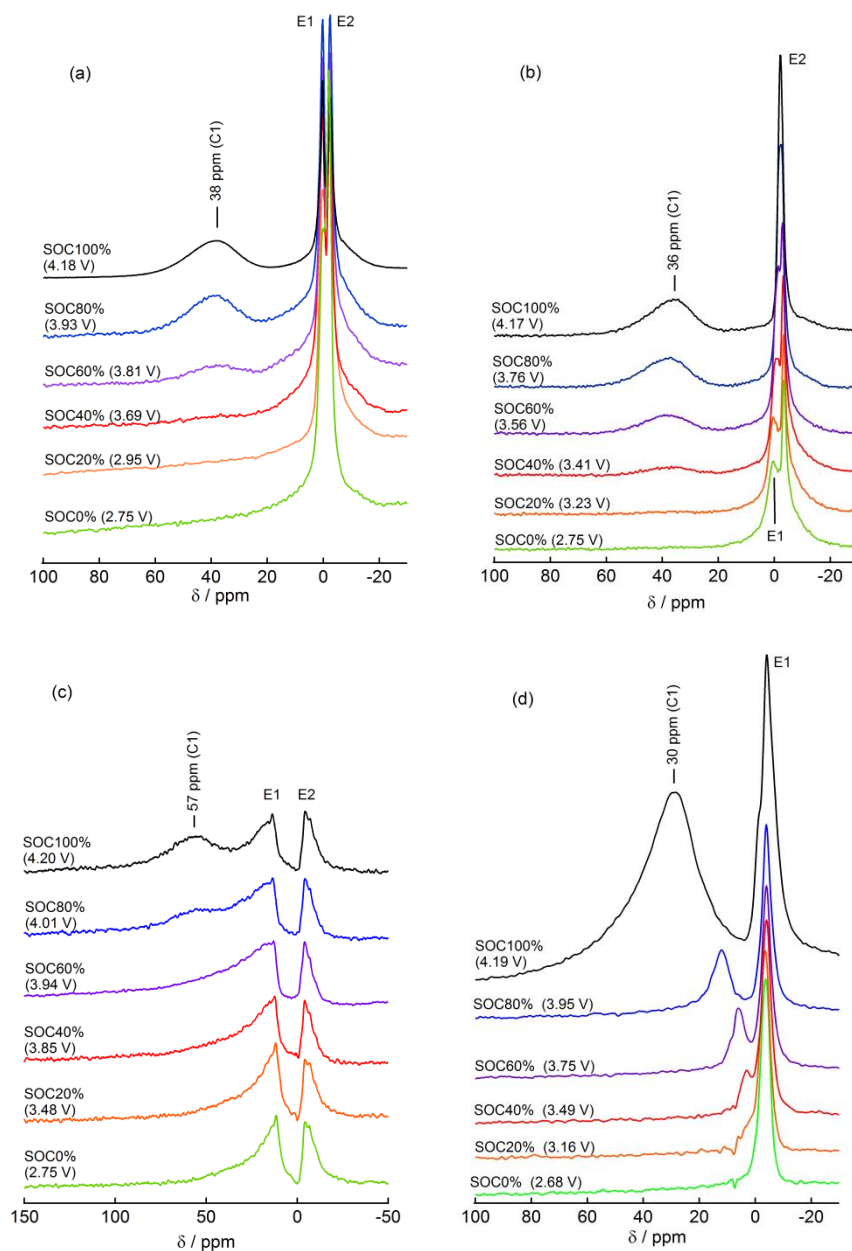
Fig. 3 ^{7}Li NMR spectra of LCO-gph (a), NCA-gph (b), LMO-gph (c), and LCO-hc (d) cells.

A broad background signal, which is ascribed to positive electrode, and the other narrower signals were observed in each NMR spectrum. Although the signals of $LiCoO_2$ in LCO-gph and LCO-hc (broad background signals in Figs. 3(a)(d) and Figs. S1(a)(d) around +220 to -200 ppm) overlapped with the other peaks, each narrow peak was distinguished

9

definitively because of the extraordinarily different line widths. The narrow components in the NCA-gph spectra (Fig. 3(b)) and LMO-gph (Fig. 3(c)) were also distinguished clearly. The spectra of LCO-gph have three narrow peaks (C1, E1 and E2) at 38, 0.2, and -2.5 ppm. The component C1 intensity decreased with the decreasing of SOC and disappeared under SOC = 40%. Therefore, it was assigned to the signal of first or second stage Li - graphite (LiC_6 or LiC_{12}) of the negative electrode, although LiC_6 and LiC_{12} generally show peaks respectively at 42 and 44 ppm. Indeed, the reduction of the C1 signal is in good agreement with previous studies on a half cell [9, 10] although quadrupolar satellites are not observed in our spectra. The components E1 and E2 should be assigned to the electrolyte because of the narrowness of the signal. The two signals might reflect the Li in electrolyte solution and Li on the surface of positive electrodes. Further study must be done to clarify this point. NCA-gph spectra (Fig. 3(b)) also included intercalated Li (LiC_6 or LiC_{12}) in negative electrode (C1), and two peaks (E1 and E2) at the SOC under 60%. However, the peaks E1 and E2 did not split at the SOC over 60%; a sharp peak was observed. The shapes of LMO-gph spectra (Fig. 3(c)) differed considerably from the former two spectra. The peak shift of intercalated Li (C1) was 57 ppm. The widths of E1 and E2 were larger than those of the other samples (Fig. 3(a) and 3(b)). The shift of the peaks (C1, E1, and E2) and the broadening of the peaks (E1 and E2) are explained by an influence of magnetic susceptibility of LMO in positive electrodes. Our NMR results revealed that the magnetic susceptibility of LMO affects the chemical shift and the peak shape not only of Li in electrolyte solution but also of the counter electrode in the *in situ* cell. Indeed, it has been reported that ^{7}Li MAS NMR of LMO observed a broad signal at about 600 ppm [21], and it

shifted depending on the angle between static magnetic field (B_0) and the sample because of its stronger bulk magnetic susceptibility [17, 18].
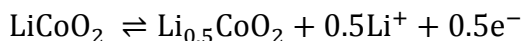
LCO-hc cell (Fig. 4(d)) showed two peaks at 30 and -4 ppm at SOC 100%. The former, which is ascribed to Li doped in hard carbon, shifted to a lower frequency with discharging. The result is consistent with our previous NMR experiments [4].

3.3 *Absorption ability of deposited Li-metal by carbon materials in negative electrode*
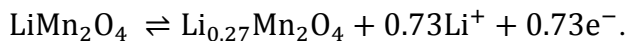
The temporal variations of ^{7}Li NMR spectrum in the LCO-gph, NCA-gph, and LCO-hc cells after overcharging at 170% of SOC by 2 C are shown in Figs. 4–6. Spectra of a LMO-gph cell are not shown because the signal of Li metal could not be observed after overcharging. Figure 4 shows the first spectrum of each cell immediately after overcharging. Figure 5 displays the temporal variations of the spectra given in Fig. 4. Signals assignable to deposited Li metal were observed at around 260 ppm in three samples. The signals decreased over time, which clearly indicates a "relaxation effect" by carbon electrodes: an absorption effect of deposited Li metal on the surface of negative electrode into the carbon. Figures 6(a)–6(c) are temporal variations of ^{7}Li NMR signals ascribed to Li metal in LCO-gph (a), NCA-gph (b), LCO-hc (c). Figures 7(a) −7(c) are time dependences of the intensities of Li metal signals and stored Li signals in carbon. The signal intensities of Li metal and Li in carbon were successfully estimated by fitting using Gaussian and Lorentzian curves, respectively. The intensity of the Li metal signal in LCO-gph was 76% of that of the Li signal in carbon just after the end of overcharge, and then it decreased rapidly during the first few hours. Then it gradually weakened during the subsequent several hours (Figs. 5(a), 6(a) and 7(a)). After 8 h, the intensity became constant at about

42% of the initial intensity. The signal of intercalated lithium (38 ppm) in graphite increased inversely proportional to the Li metal signal (Figs. 5(a), 6(a) and 7(a)). The result illustrates the relaxation effect of Li metal occurs by transfer of lithium into graphite electrode. It is particularly interesting that a slight shift of the peak of the Li metal signal from 260 ppm to 265 ppm with elapsed time was observed (Fig. 6(a)). Chandrashekar et al. reported that microstructural lithium deposited on Li metal electrode has a lower chemical shift [22]. The ablation of lower-shift component in Li metal suggests that the lithium metal having microstructure such as dendritic structure can be re-dissolved more easily and that it diffuses into the electrode rapidly, whereas larger Li metal particles remain on the surface of the electrode, even after 14.2 h.

NCA-gph also exhibited a reduction of Li metal signal, although the decrement was only ca. 20%; most of the reduction occurred only in the first 17 min (Figs. 6(b) and 7(b)). The intensity of deposited Li metal was much less than that of LCO-gph. That fact is explainable by the composition of positive electrodes. Generally, LCO electrodes can react reversibly under 4.2 V. The reaction is described as shown below.

$$LiCoO_2 \rightleftharpoons Li_{0.5}CoO_2 + 0.5Li^+ + 0.5e^-$$

Therefore, about 50% of the lithium remains in the positive electrode even at 100% of SOC. The remaining lithium moves to the negative electrode by overcharging over 4.2 V, and thereafter precipitates on the negative electrode surface as Li metal. However, NCA and LMO electrodes have less lithium in their crystal structures at 100% of SOC. Ohzuku et al. reported [23] that the composition of LMO in a LIB cell at 4.2 V was estimated as $Li_{0.27}Mn_2O_4$. The reaction is

$$LiMn_2O_4 \rightleftharpoons Li_{0.27}Mn_2O_4 + 0.73Li^+ + 0.73e^-.$$

In fact, for NCA, it was also estimated that only approximately 20% of Li remains in the positive electrode. The peak intensity of Li stored in graphite in the NCA-gph cell also seems to increase gradually (Fig. 7(b)) between 4 and 8 h, as does LCO-gph. Although the reason remains unclear, another process of lithium intercalation is implied.

In the ^{7}Li NMR spectrum of LCO-hc after overcharging, clear signals of Li metal (263 ppm), stored lithium in the hard carbon which consists of lithium in closed pores and between graphene layers (40–140 ppm), and lithium in electrolyte (-4 ppm) were observed (Fig. 4(c)). The intensity of the deposited Li metal signal was only 23% of that of the Li signal in carbon just after the overcharging, and 80% of the Li metal signal disappeared after 8.5 h (Figs. 6(c) and 7(c)). The stored lithium showed a peak at 80 ppm and a shoulder structure at about 100–120 ppm at first, but the shoulder structure faded over time (Figs. 6(d) and 7(c)). That fading is explainable by progression to an equilibrium state by lithium diffusion in carbon. Lithium was stored densely near the carbon particle surface immediately after the overcharging, although lithium was sparse in the carbon particle center. The state must be homogenized during the subsequent 10–15 h. The smaller initial intensity and the greater relaxation effect on deposited Li metal than on graphite is ascribed to the structure of the hard carbon containing lots of closed pores. The negative electrode in the cell still had a margin to accommodate lithium ions with closed pores in hard carbon. In these experiments, we overcharged the cell by CC mode without CV. Presumably, most of the deposited lithium atoms were partially oxidized again and transferred into carbon, and stored as quasimetallic lithium. Indeed, the signal intensity of lithium stored in carbon (40–140 ppm) increased 17% between the initial spectrum and the last spectrum after 14.7 h.
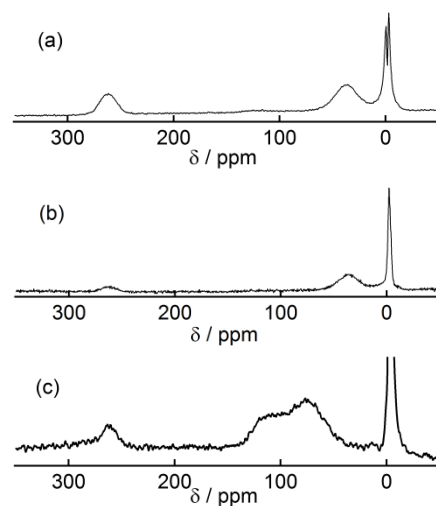
Fig. 4 ^{7}Li NMR spectra of LCO-gph (a), NCA-gph (b), and LCO-hc (c) cells after overcharging to 170 % SOC by 2 C.
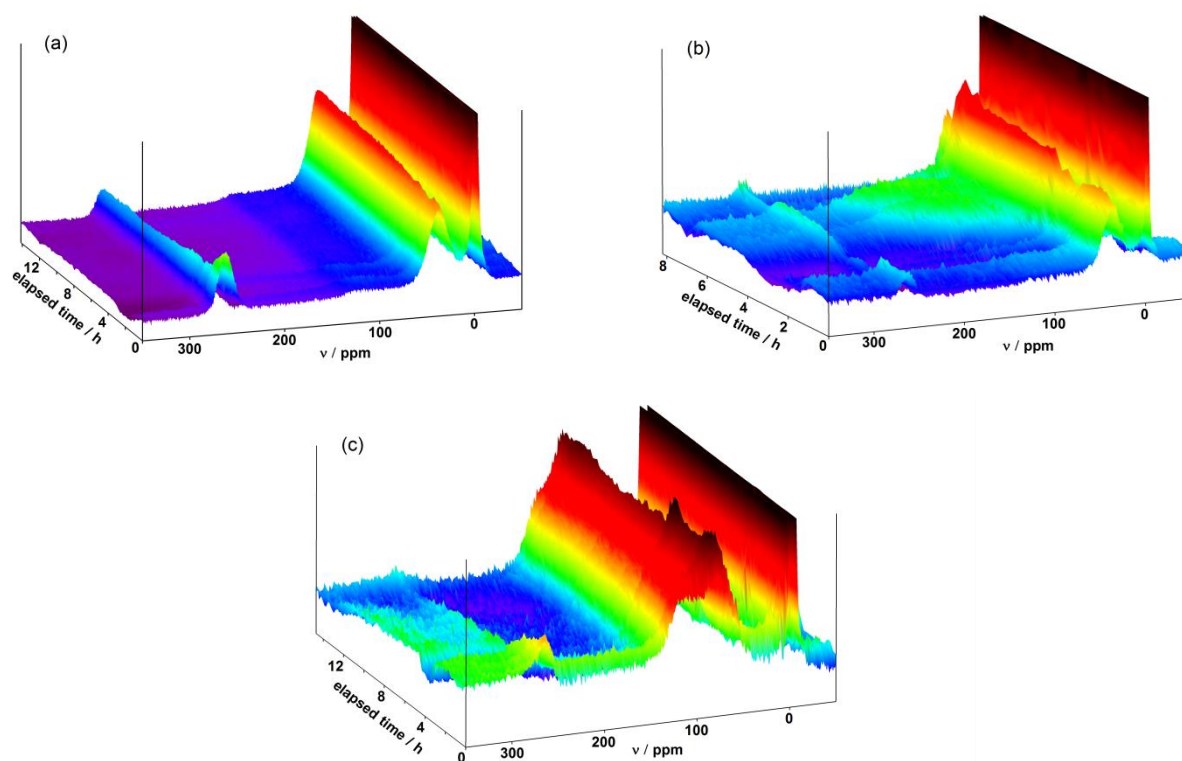

Fig. 5   Temporal variations of ^{7}Li NMR spectra of LCO-gph (a), NCA-gph (b), and LCO-hc (c) cells after overcharging.
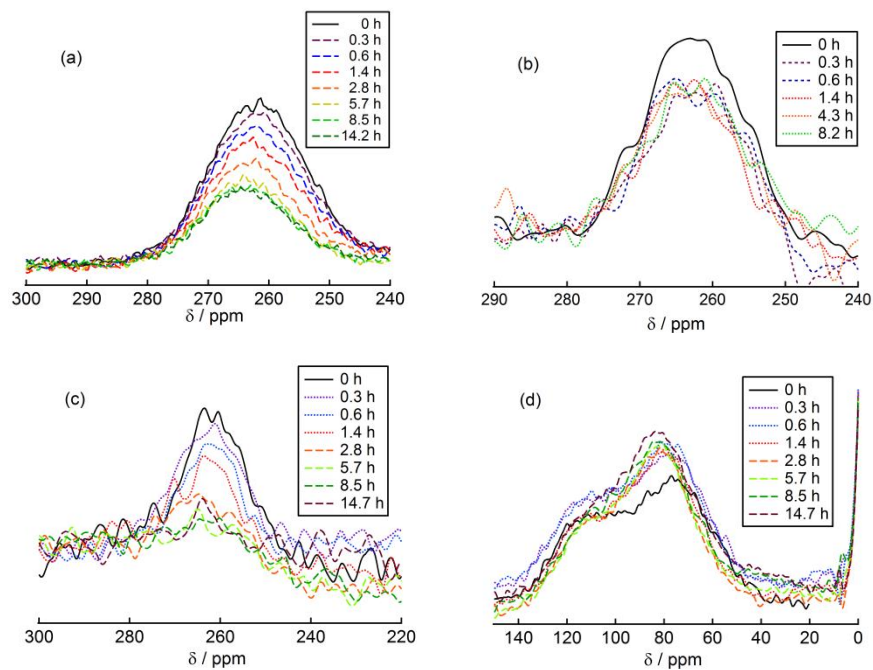
14

Fig. 6   Temporal variations of ^{7}Li NMR signals ascribed to Li metal in LCO-gph (a), NCA-gph (b), LCO-hc (c), and a signal for stored lithium in hard carbon in LCO-hc (d).
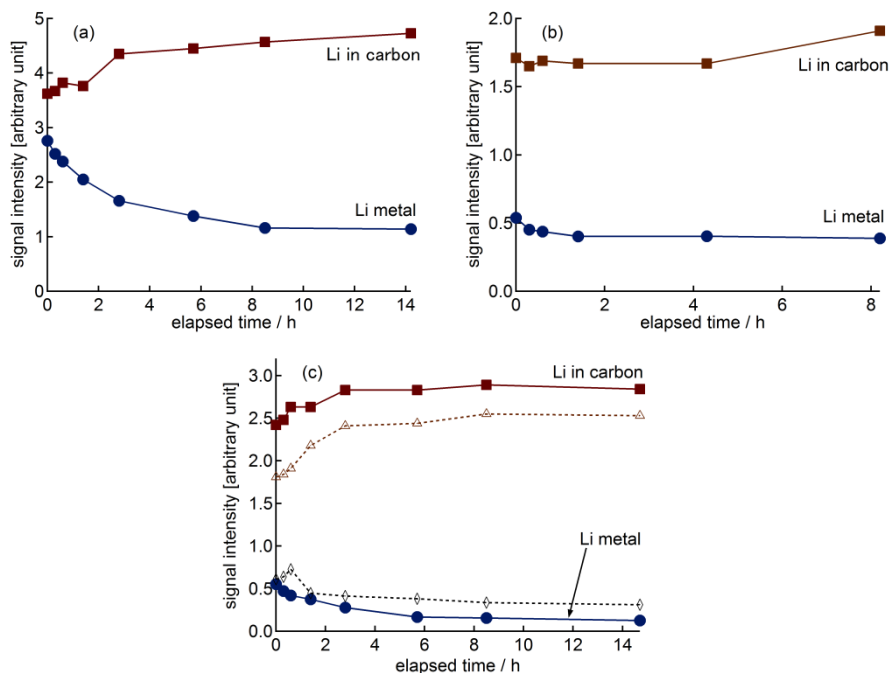
Fig. 7　Temporal variations of ^{7}Li NMR signal intensities. Two signal components in overcharged LCO-gph spectrum (Figs. 5(a),6(a)), NCA-gph (Fig. 5(b),6(b)), and LCO-hc (Figs. 5(c),5(d),6(c),6(d)), are displayed in (a), (b), and (c), respectively. Li metal signals are denoted by filled circles (●), whereas signals for stored lithium in carbon are shown by filled squares (■). Open triangles and open rhombuses in Fig. 7(c) denote respectively signal intensities of the main peaks and shoulder structures of stored lithium in carbon (filled squares).

The relaxation effect of the deposited metal Li-dendrite on negative electrode has never been reported in the relevant literature, although it has long been suggested. In this study, we directly observed the reduction of Li metal on the electrode and evaluated the rate of transfer of lithium into carbon using *in situ* NMR technique. The results are expected to be extremely important for discussion of the state of lithium, and for the safe design of new batteries. The deposition of the lithium dendrite depends not only on the composition of the positive electrode (lithium content) and the structure of carbon in the negative electrode, but also on the diffusion rate of lithium in each component of the cell. Experiments

conducted at high/low temperature and/or high charging rates are currently proceeding toward the use of the battery for large devices such as electric vehicles or storage systems of electricity for houses or infrastructure.

4. Conclusion

In situ ^{7}Li NMR experiments were feasible for the lithium ion cells arranged for practical use, i.e., the cells using the Cu and Al foils, and coated by the Al-deposited laminate film. Reduction in the NMR signal intensity attributable to RF shielding was 60–65% compared to the samples without the foils and the Al-laminate film. The cells used for *in situ* NMR experiments were stable. They only slightly degraded during three months in the atmosphere. The magnetic susceptibility of lithium metal oxide included in the positive electrodes affected the position of the ^{7}Li peaks coming from the negative electrodes and electrolyte.

The ^{7}Li NMR spectra in the LCO-gph, NCA-gph, and LCO-hc cells after overcharging at 170% of SOC by 2 C or 3C showed signs of deposited Li metal at around 260 ppm, although LMO-gph showed no such signals. The Li metal signals decreased with time because of absorption into the carbon. The effect occurs rapidly in a first few hours, but reaches an equilibrium state in 8–15 h. The slight shift of the deposited metal peak suggests that dendritic Li easily re-dissolves, although the larger particles remain. The hard carbon electrode has a larger effect of Li metal relaxation than graphite electrodes, as explained by the bufferable structure of the carbon: closed pores. We showed that the use of *in situ* NMR to observe actual component cells is a prominent means to evaluate the safety of various LIBs against overcharging.

17

References

[1] Yoshio M, Brodd RJ, Kozawa A, eds. Lithium-ion batteries; science and technologies. LaVergne: Springer 2009.

[2] Conard J, Lauginie P. Lithium NMR in lithium–carbon solid state compounds. Tanso 2000;191:62–70.

[3] Grey CP, Dupré N. NMR studies of cathode materials for lithium-ion rechargeable batteries. Chem Rev 2004;104(10):4493–512.

[4] Gotoh K, Maeda M, Nagai A, Goto A, Tansho M, Hashi K et al. Properties of a novel hard-carbon optimized to large size Li ion secondary battery studied by ^{7}Li NMR. J Power Sources 2006;162(2):1322–8.

[5] Fujimoto H, Mabuchi A, Tokumitsu K, Chinnasamy N, Kasuh T. ^{7}Li nuclear magnetic resonance studies of hard carbon and graphite/hard carbon anode for Li ion battery. J Power Sources 2011;196(3):1365–70.

[6] Blanc F, Leskes M, Grey CP. *In situ* solid-state NMR spectroscopy of electrochemical cells: batteries, supercapacitors, and fuel cells. Accounts Chem Res 2013;46(9):1952–63.

[7] Kuwata N, Iwai Y, Kawamura J. Research and development of lithium-ion battery using laser and nuclear magnetic resonance. Materials Integration 2011;24(4, 5):172–9.

[8] Trease NM, Köster TKJ, Grey CP. *In situ* NMR studies of lithium ion batteries. Electrochem Soc Interface 2011;20(3):69–73.

[9] Chevallier F, Poli F, Montigny B, Letellier M. *In situ* [7]Li nuclear magnetic resonance observation of the electrochemical intercalation of lithium in graphite: second cycle analysis. Carbon 2013;61:140–53.

[10] Letellier M, Chevallier F, Morcrette M. *In situ* [7]Li nuclear magnetic resonance observation of the electrochemical intercalation of lithium in graphite: First cycle. Carbon 2007;45(5):1025–34.

[11] Letellier M, Chevallier F, Béguin F. *In situ* ^{7}Li NMR during lithium electrochemical insertion into graphite and a carbon/carbon composite. J Phys Chem Solid 2006;67(5–6):1228–32.

[12] Letellier M, Chevallier F, Béguin F, Frackowiak E, Rouzaud J-N. The first *in situ* ^{7}Li NMR study of the reversible lithium insertion mechanism in disorganised carbons. J Phys Chem Solid 2004;65(2–3):245–51.

[13] Letellier M, Chevallier F, Clinard C, Frackowiak E, Rouzaud J-N, Béguin F et al. The first *in situ* [7]Li nuclear magnetic resonance study of lithium insertion in hard-carbon anode materials for Li-ion batteries. J Chem Phys 2003;118(13):6038–45.

[14] Ogata K, Salager E, Kerr CJ, Fraser AE, Ducati C, Morris AJ et al. Revealing lithium–silicide phase transformations in nano-structured silicon-based lithium ion batteries via *in situ* NMR spectroscopy. Nature Comm 2014;5:4217/1–/11. DOI: 10.1038/ncomms4217

[15] Key B, Bhattacharyya R, Morcrette M, Seznéc V, Tarascon JM, Grey CP. Real-time NMR investigations of structural changes in silicon electrodes for lithium-ion batteries. J Am Chem Soc 2009;131(26):9239–49.

[16] Shimoda K, Murakami M, Takamatsu D, Arai H, Uchimoto Y, Ogumi Z. *In situ* NMR observation of the lithium extraction/insertion from $LiCoO_2$ cathode. Electrochim Acta 2013;108:343–9.

[17] Trease NM, Zhou L, Chang HJ, Zhu BY, Grey CP. *In situ* NMR of lithium ion batteries: Bulk susceptibility effects and practical considerations. Solid State Nucl Magn Reson 2012;42:62–70.

[18] Zhou L, Leskes M, Ilott AJ, Trease NM, Grey CP. Paramagnetic electrodes and bulk magnetic susceptibility effects in the *in situ* NMR studies of batteries: Application to $Li_{1.08}Mn_{1.92}O_4$ spinels. J Magn Reson 2013;234:44–57.

[19] Gotoh K, Ueda T, Omi H, Eguchi T, Maeda M, Miyahara M et al. Observation of micropores in hard-carbon using ^{129}Xe NMR porosimetry. J Phys Chem Solids 2008;69(2):147–52.

[20] Takeda K. OPENCORE NMR: Open-source core modules for implementing an integrated FPGA-based NMR spectrometer. J Magn Reson 2008;192(2):218–29.

[21] Mustarelli P, Massarotti V, Bini M, Capsoni D. Transferred hyperfine interaction and structure in $LiMn_2O_4$ and Li_2MnO_3 coexisting phases: A XRD and ^7Li NMR–MAS study. Phys Rev B 1997;55(18):12018–24.

[22] Chandrashekar S, Trease NM, Chang HJ, Du LS, Grey CP, Jerschow A. ^7Li MRI of Li batteries reveals location of microstructural lithium. Nat Mater 2012;11(4):311–5.

[23] Ohzuku T, Kitagawa M, Hirai T. Electrochemistry of manganese dioxide in lithium nonaqueous cell. III. X-ray diffractional study on the reduction of spinel-related manganese dioxide. J Electrochem Soc. 1990;137(3):769–75.